Journal of the Optical Society of America B

OPTICAL PHYSICS

Force on an electric dipole near an ENZ interface

Henk F. Arnoldus* and Zhangjin Xu

Department of Physics and Astronomy, Mississippi State University, P.O. Box 5167, Mississippi State, Mississippi 39762, USA
*Corresponding author: hfa1@msstate.edu

An electric dipole near a surface is subject to the electromagnetic force by its own reflected field. We have derived a closed-form expression for this force for the case of an epsilon-near-zero (ENZ) medium. This force is perpendicular to the surface, and it is repulsive. We show that this force is due to the evanescent reflected field. For a rotating dipole moment, there is also a lateral force, which, in the ENZ limit, is vanishing small. However, when a small amount of damping is present in the material, this force becomes comparable with the force component perpendicular to the surface.   © 2019 Optical Society of America

https://doi.org/10.1364/JOSAB.36.000F18

1. INTRODUCTION

Epsilon-near-zero materials are impenetrable materials for radiation in the usual sense. When a plane electromagnetic wave is incident on an ENZ interface, it creates a wave in the medium that travels along the surface and decays exponentially in amplitude in the direction away from the surface. For close to normal incidence, however, the electric component of the field extends into the medium, but the corresponding magnetic field is zero. This electric field oscillates with the frequency of the incident wave, but it has no spatial dependence. This bizarre phenomenon is referred to as "static optics." There is no energy flow into the material associated with this penetration of the electric field (Poynting vector is zero). The polarization of this electric field is the same as the polarization of the incident field (assumed to be s or p). However, for p polarization, and just off normal incidence, the polarization of the electric field becomes circular [1].

When the relative permittivity ε_r of the medium vanishes, so does the index of refraction n because $n = \sqrt{\varepsilon_r}$. The Green's function for wave propagation is $g(r) = \exp(ink_o r)/r$, with $k_o = \omega/c$ the wavenumber in free space, and ω is the angular frequency of the radiation. For an ENZ medium, this becomes $g(r) = 1/r$, which is the Green's function of electrostatics. An oscillating electric field may exist in the medium, but there is no spatial dependence or retardation. As a result, an electric field can be squeezed or funneled through such a material [2–7] without loss of phase information. Due to the sharp, almost discontinuous, behavior near normal incidence, such materials can be used for angular filtering of radiation [8–11]. Enhancement of the magneto-optical effect [12] is another prediction. Metamaterials are artificial, subwavelength structures, designed in such a way that they effectively (macroscopically) behave as continuous media. The goal is then to design structures that behave as continuous ENZ media. Early attempts

were restricted to low-frequency radiation [13–17], but, more recently, ENZ materials have been fabricated for the optical region of the spectrum [18–20].

Properties of atoms, molecules, and nanoparticles are modified when they are close to the interface with a medium. Early experiments by Drexhage [21] showed that emission rates by molecules are affected by the presence of a dielectric interface, and their radiation patterns are drastically altered due to interference between directly emitted radiation and the reflected radiation by the interface. Another direct consequence of the medium is that the reflected light exerts a force on the particle. For a common dielectric or metal, this is an attractive force, which tends to make the particle stick to the surface. It has been predicted [22,23] that, near an ENZ interface, this force may be repulsive, leading to possible levitation of the particle. It has been argued [24] that this is due to the expulsion of the electromagnetic field by the material, in analogy to the Meissner effect for superconductors. We shall consider this force, and derive an explicit expression for it, for any state of oscillation of the dipole. It will be shown that the force is (almost) entirely due to reflected evanescent waves. We shall also show that the force is due to the phase shift upon reflection by the ENZ medium rather than due to expulsion of the radiation by the material.

2. FORCE ON AN ELECTRIC DIPOLE

An electric dipole moment, oscillating at angular frequency ω, can be represented as

$$\mathbf{d}(t) = \text{Re}[\mathbf{d}\ \exp(-i\omega t)]. \tag{1}$$

Here, $\mathbf{d}$ is the complex amplitude of the dipole moment $\mathbf{d}(t)$. This dipole moment will usually be induced through irradiation by a laser, oscillating at angular frequency ω. The magnitude of vector $\mathbf{d}$ depends on the laser power. For linear laser

polarization, vector $\mathbf{d}$ is real, and $\mathbf{d}(t)$ oscillates linearly. For circular or elliptic polarization, vector $\mathbf{d}$ is complex, and $\mathbf{d}(t)$ traces out a circle or an ellipse in a plane. For a dipole near an interface, as considered below, $\mathbf{d}$ can also have contributions due to the presence of reflected light. Here, we shall take $\mathbf{d}$ as given. The oscillating dipole emits electromagnetic radiation, and the electric field must therefore have the form

$$\mathbf{E}(\mathbf{r}, t) = \text{Re}[\mathbf{E}(\mathbf{r}) \exp(-i\omega t)], \tag{2}$$

with $\mathbf{E}(\mathbf{r})$ the complex amplitude. The magnetic field $\mathbf{B}(\mathbf{r}, t)$ oscillates similarly. When the dipole is located at $\mathbf{r}_o$ and is subject to an electric and magnetic field, the time-averaged force on the dipole is given by [25]

$$\mathbf{F} = \frac{1}{2}\text{Re}[(\mathbf{d}^* \cdot \nabla)\mathbf{E}(\mathbf{r}) + i\omega\mathbf{d}^* \times \mathbf{B}(\mathbf{r})]_{\mathbf{r}=\mathbf{r}_o}. \tag{3}$$

The first term is the Coulomb force by the electric field, and the second term is the Lorentz force by the magnetic field. For time-harmonic fields, the magnetic field follows from the electric field according to Faraday's law:

$$\mathbf{B}(\mathbf{r}) = -\frac{i}{\omega}\nabla \times \mathbf{E}(\mathbf{r}), \tag{4}$$

and this allows for the elimination of the magnetic field from Eq. (3). We then obtain

$$\mathbf{F} = \frac{1}{2}\text{Re}[\nabla(\mathbf{d}^* \cdot \mathbf{E}(\mathbf{r}))]_{\mathbf{r}=\mathbf{r}_o}, \tag{5}$$

which offers a great computational simplification, as compared with Eq. (3).

3. DIPOLE NEAR AN INTERFACE

An electric dipole is located a distance H above an interface with a medium, as illustrated in Fig. 1. We take the dipole to be on the z axis, and the interface is the x–y plane. The medium shown is a half-infinite dielectric, although that is irrelevant at this stage.

The dipole emits radiation, and this radiation is reflected at the surface. A most convenient representation of this reflected radiation is by means of an angular spectrum. It can be shown that [26]

$$\mathbf{E}_r(\mathbf{r}) = \frac{ik_o}{8\pi^2\varepsilon_o}\sum_\sigma \int d^2\mathbf{k}_\parallel \frac{e^{ihv_1}}{v_1}(\mathbf{d} \cdot \mathbf{e}_{\sigma,i})R_\sigma\mathbf{e}_{\sigma,r}e^{i\mathbf{k}_r \cdot \mathbf{r}}, \tag{6}$$

which holds without approximation. The spectrum is a superposition of polarized ($\sigma = s$, p) plane reflected waves, and the integration runs over the $\mathbf{k}_\parallel$ plane. The wave vector of
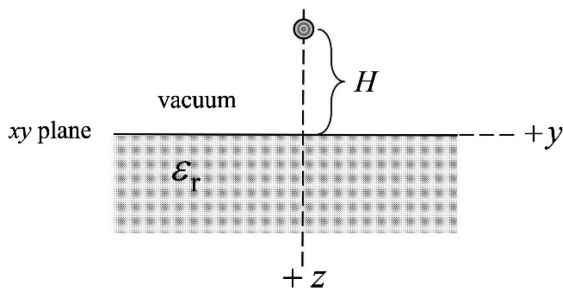

Fig. 1. Illustration of an electric dipole near a dielectric interface.

the reflected wave is $\mathbf{k}_r = \mathbf{k}_\parallel - k_o v_1 \mathbf{e}_z$. The unit vector in the $\mathbf{k}_\parallel$ direction is $\hat{\mathbf{k}}_\parallel$, and, for the magnitude of the vector, we write $k_\parallel = \alpha k_o$. We have introduced $h = k_o H$ as the dimensionless distance between the surface and the dipole. The unit polarization vectors for the incident (i) and reflected (r) fields are chosen as

$$\mathbf{e}_{s,i} = \mathbf{e}_{s,r} = \mathbf{e}_z \times \hat{\mathbf{k}}_\parallel, \tag{7}$$

$$\mathbf{e}_{p,i} = \alpha\mathbf{e}_z - v_1\hat{\mathbf{k}}_\parallel, \tag{8}$$

$$\mathbf{e}_{p,r} = \alpha\mathbf{e}_z + v_1\hat{\mathbf{k}}_\parallel. \tag{9}$$

Here,

$$v_1 = \sqrt{1 - \alpha^2}, \tag{10}$$

which has the significance of the dimensionless z component of the wave vector of the incident wave. For $0 \le \alpha < 1$, v_1 is positive, and both incident and reflected waves are traveling waves. For $1 < \alpha < \infty$, v_1 is positive imaginary, and both the incident wave and the reflected wave are evanescent. They decay exponentially in the directions away from the surface. The R_s and R_p are the Fresnel reflection coefficients for s- and p-polarized waves, respectively. They depend on the variable $\mathbf{k}_\parallel$ through its magnitude parameter α, but they do not depend on the direction of $\mathbf{k}_\parallel$. Expressions for these coefficients can be obtained from the appropriate boundary conditions at the interface.

For a single interface with a dielectric, as in Fig. 1, the Fresnel coefficients are

$$R_s = \frac{v_1 - v_3}{v_1 + v_3}, \tag{11}$$

$$R_p = \frac{\varepsilon_r v_1 - v_3}{\varepsilon_r v_1 + v_3}, \tag{12}$$

with

$$v_3 = \sqrt{\varepsilon_r - \alpha^2}, \tag{13}$$

as the dimensionless z component of the wave vector of the transmitted wave.

4. EVALUATION OF THE FORCE

The force on the dipole is exerted by its own reflected field. Expression (6) for $\mathbf{E}_r(\mathbf{r})$ is substituted into Eq. (5) for the force. The gradient brings down the reflected wave vector as $i\mathbf{k}_r$. We adopt polar coordinates $(k_\parallel, \tilde{\phi})$ in the $\mathbf{k}_\parallel$ plane. Then, we have $\mathbf{k}_\parallel = \alpha k_o(\mathbf{e}_x \cos\tilde{\phi} + \mathbf{e}_y \sin\tilde{\phi})$, and the polarization vectors from Eqs. (7) to (9) can be expressed in terms of $\tilde{\phi}$. The integrations over $\tilde{\phi}$ in the numerous terms are elementary. For the complex amplitude of the dipole moment, we set $\mathbf{d} = d_o\hat{\mathbf{u}}$, with $d_o > 0$, and vector $\hat{\mathbf{u}}$ is normalized as $\hat{\mathbf{u}}^* \cdot \hat{\mathbf{u}} = 1$. After regrouping, the expression for the force near an interface can be written in the attractive form

$$\mathbf{F} = f_o[(\hat{\mathbf{u}}_\perp^* \cdot \hat{\mathbf{u}}_\perp)v_\perp(h) + (\hat{\mathbf{u}}_\parallel^* \cdot \hat{\mathbf{u}}_\parallel)v_\parallel(h)]\mathbf{e}_z$$
$$+ f_o v_\times(h)\text{Im}[(\hat{\mathbf{u}}^* \cdot \mathbf{e}_z)\hat{\mathbf{u}}_\parallel]. \tag{14}$$

Here, the overall constant

$$f_o = \frac{d_o^2 k_o^4}{8\pi\varepsilon_o} \tag{15}$$

is a measure for the strength of the force. The three functions of h appearing in Eq. (14) are

$$v_{\perp}(h) = \text{Re} \int_0^{\infty} d\alpha \alpha^3 e^{2ihv_1} R_p(\alpha), \qquad (16)$$

$$v_{\parallel}(h) = \frac{1}{2} \text{Re} \int_0^{\infty} d\alpha \alpha e^{2ihv_1} [R_s(\alpha) - (1 - \alpha^2) R_p(\alpha)], \qquad (17)$$

$$v_{\times}(h) = -\text{Im} \int_0^{\infty} d\alpha \alpha^3 e^{2ihv_1} R_p(\alpha). \qquad (18)$$

Equation (14) holds for any state of oscillation of the dipole, and no properties of the Fresnel coefficients have been used (other than rotational symmetry around the surface normal). For a perpendicular dipole, we have $\hat{\mathbf{u}} = \mathbf{e}_z$, and Eq. (14) reduces to $\mathbf{F} = f_o v_{\perp}(h) \mathbf{e}_z$. The force is along the surface normal, either up or down, depending on the sign of $v_{\perp}(h)$. Similarly, for a parallel dipole, the force is $\mathbf{F} = f_o v_{\parallel}(h) \mathbf{e}_z$. In general, a dipole moment will have a perpendicular and parallel component, and Eq. (14) shows how these mix. Interestingly, there also appears a cross term containing the function $v_{\times}(h)$. For this term to contribute, the vector $\hat{\mathbf{u}}$ must have both a perpendicular and a parallel component, and it has to be complex. For instance, for

$$\hat{\mathbf{u}} = -\frac{1}{\sqrt{2}} (\mathbf{e}_y + i\mathbf{e}_z), \qquad (19)$$

we have a dipole moment rotating in the y–z plane, and such that the dipole moment $\mathbf{d}(t)$ rotates counterclockwise when viewed down the positive x axis. For the setup in Fig. 1, this is clockwise. Then, $\text{Im}[(\hat{\mathbf{u}}^* \cdot \mathbf{e}_z)\hat{\mathbf{u}}_{\parallel}] = -\mathbf{e}_y/2$. There is a lateral force along the surface, along the y axis, which is in the plane of rotation. The direction of the force depends on the sign of $v_{\times}(h)$. Such a lateral force on rotating dipoles has been predicted recently [27].

5. FORCE NEAR AN ENZ INTERFACE

For an ENZ material, we have $\varepsilon_r = 0$, and the Fresnel coefficients from Eqs. (11) and (12) simplify to

$$R_s = \left(\sqrt{1 - \alpha^2} - i\alpha \right)^2, \qquad (20)$$

$$R_p = -1. \qquad (21)$$

For this case, the functions $\nu_i(h)$ become universal functions of h in the sense that there is no dependence on any other parameters left. For an ENZ material, the integrals in Eqs. (16)–(18) can be evaluated explicitly, as we shall now show.

In order to evaluate the integrals over α, we split them into integrals over the range $0 \leq \alpha < 1$ and over the range $1 < \alpha < \infty$. For the first range, the corresponding reflected waves are traveling waves; for the second range, the reflected waves are evanescent. The functions split accordingly, as for instance $v_{\perp}(h) = v_{\perp}(h)^{\text{tr}} + v_{\perp}(h)^{\text{ev}}$. For $0 \leq \alpha < 1$, we make the substitution $t = (1 - \alpha^2)^{1/2}$; for $1 < \alpha < \infty$, we set $t = (\alpha^2 - 1)^{1/2}$. For $v_{\perp}(h)$, we obtain

$$v_{\perp}(h) = \frac{2}{\beta^2} \left[\left(1 - \frac{3}{\beta^2} \right) \cos \beta - \frac{3}{\beta} \sin \beta \right], \qquad (22)$$

where we have set $\beta = 2h$. For the cross term, we obtain

$$v_{\times}(h) = -\frac{2}{\beta^2} \left[\frac{3}{\beta} \cos \beta + \left(1 - \frac{3}{\beta^2} \right) \sin \beta \right]. \qquad (23)$$

The result for $v_{\parallel}(h)$ is somewhat more complicated. We find

$$v_{\parallel}(h) = \frac{1}{\beta^2} \left(4 - \frac{9}{\beta^2} \right) \cos \beta + \frac{1}{\beta} \left(1 - \frac{9}{\beta^2} \right) \sin \beta + \frac{1}{15} \beta + L(\beta)$$
$$+ \frac{\pi}{2\beta^2} (\mathbf{H}_2(\beta) - \beta \mathbf{H}_3(\beta)). \qquad (24)$$

Here, we introduced

$$L(\beta) = \int_0^{\infty} dt t^2 \sqrt{1 + t^2} e^{-\beta t}, \qquad (25)$$

and this function is shown in Fig. 2 as a function of h. The Struve functions are defined as [28]

$$\mathbf{H}_n(\beta) = \left(\frac{\beta}{2} \right)^{n+1} \sum_{k=0}^{\infty} \frac{(-1)^k}{\Gamma(k + 3/2)\Gamma(k + n + 3/2)} \left(\frac{\beta}{2} \right)^{2k}. \qquad (26)$$

The functions $v_{\perp}(h)$, $v_{\parallel}(h)$, and $v_{\times}(h)$ are shown in Fig. 3. These functions, together with the dipole orientation vector $\hat{\mathbf{u}}$, determine the force on the dipole near the ENZ interface, apart from the overall constant f_o. The functions $v_{\perp}(h)$ and $v_{\parallel}(h)$ are seen to be negative, except for small wiggles at large distances. This means that the force is repelling and upward in Fig. 1. Because gravity is down, this force by the reflected field can give rise to levitation of the particle, holding it in suspension at a certain distance above the interface, as predicted in [24]. This will be a stable equilibrium. When the particle would move up a little, the electromagnetic force gets weaker,
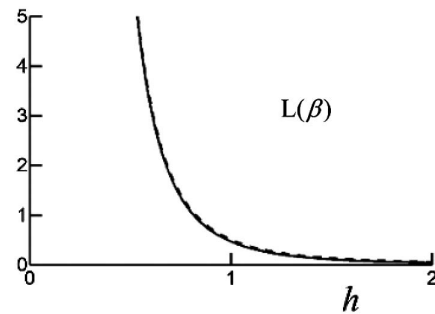
Fig. 2. Shown is the function $L(\beta)$ (solid line) as a function of h and its approximation by two terms (dashed line).
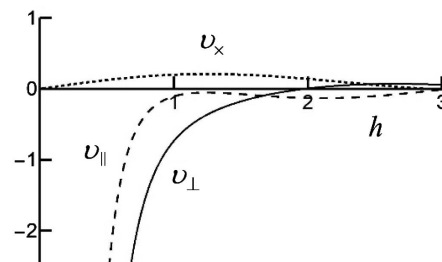
Fig. 3. Figure shows the three functions that determine the force on the dipole near an ENZ medium, as a function of h.

and gravity will pull it back to equilibrium. If the particle would move down a little, the electromagnetic repulsive force increases and will push the particle back up to equilibrium. Because $h = 2\pi$ corresponds to an optical wavelength in free space, we see that the repulsive force only extends outside the material over a fraction of a wavelength. This limits the particles to be suspended to atoms, molecules, and subwavelength nanoparticles. If the particle is a dielectric sphere, with a dipole moment induced by a moderate 50 mW CW laser, we can estimate f_o to be about 10^{-18} N. The force by gravity on this particle is also about 10^{-18} N, and levitation can be expected if the particle is close enough to the surface. We also see from the figure that the cross term is as good as negligible at short distances.

6. ROLE OF EVANESCENT WAVES

The results shown in Eqs. (22)–(24) represent the exact solution for the force on a dipole near an ENZ material. We shall now consider the contributions from the evanescent waves to these functions. These parts come from the integration range $1 < \alpha < \infty$ in Eqs. (16)–(18). We find, without approximation, that the evanescent parts are

$$v_\perp(h)^{\mathrm{ev}} = -\frac{6}{\beta^4} - \frac{1}{\beta^2}, \tag{27}$$

$$v_\parallel(h)^{\mathrm{ev}} = -\frac{9}{\beta^4} - \frac{1}{2\beta^2} + L(\beta), \tag{28}$$

$$v_\times(h)^{\mathrm{ev}} = 0. \tag{29}$$

We see from Fig. 4 that the curve for $v_\perp(h)^{\mathrm{ev}}$ is almost identical to the curve for $v_\perp(h)$. Therefore, the corresponding force is as good as determined by evanescent waves only. A similar conclusion holds for $v_\parallel(h)$, as illustrated in Fig. 5.

The appearance of the function $L(\beta)$ on the right-hand side of Eq. (28) contributes significantly to the evanescent part of $v_\parallel(h)^{ev}$. To see this, we make the substitution $u = \beta t$ in Eq. (25). Then, we expand the square root in a binomial series and integrate term by term. We then find

$$L(\beta) = \frac{6}{\beta^4} + \frac{1}{2\beta^2} + \dots. \tag{30}$$

When we substitute this in the right-hand side of Eq. (28), the terms with β^{-2} cancel, and the terms with β^{-4} combine as

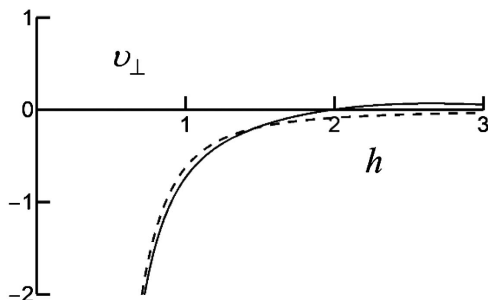$$v_\parallel(h)^{\mathrm{ev}} = -\frac{3}{\beta^4} + \dots. \tag{31}$$

Fig. 4. Figure shows $v_\perp(h)$ (solid line) and its contribution from evanescent waves (dashed line), as a function of h.
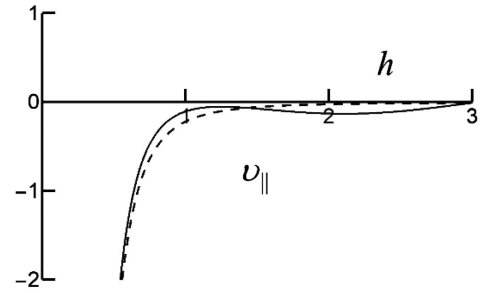

Fig. 5. Figure shows $v_\parallel(h)$ (solid line) and its contribution from evanescent waves (dashed line), as a function of h.

When graphing $-3/\beta^4$, the result is identical to the dashed curve in Fig. 5. Interestingly, the evanescent waves do not contribute to the cross term, as seen in Eq. (29).

7. CONTRIBUTIONS FROM TRAVELING WAVES

The traveling part of $v_\perp(h)$ is

$$v_\perp(h)^{\mathrm{tr}} = v_\perp(h) - v_\perp(h)^{\mathrm{ev}}, \tag{32}$$

and we find with Eqs. (22) and (27)

$$v_\perp(h)^{\mathrm{tr}} = \frac{6}{\beta^4} + \frac{1}{\beta^2} + \frac{2}{\beta^2}\left[\left(1 - \frac{3}{\beta^2}\right)\cos\beta - \frac{3}{\beta}\sin\beta\right]. \tag{33}$$

It seems that there are many negative powers of β, suggesting that $v_\perp(h)^{\mathrm{tr}}$ diverges for small β, just as $v_\perp(h)^{\mathrm{ev}}$. However, when we expand $\cos\beta$ and $\sin\beta$ in series around $\beta = 0$ and keep a large number of terms, we find that all terms with negative powers cancel exactly, and we are left with

$$v_\perp(h)^{\mathrm{tr}} = -\frac{1}{4} + \mathcal{O}(\beta^2). \tag{34}$$

Apparently, the traveling contribution is finite for β small, and $v_\perp(h)$ is determined by the diverging contribution from evanescent reflected waves.

In order to see that traveling contributions must be finite, we consider the representation

$$v_\perp(h) = -\mathrm{Re}\int_0^\infty \mathrm{d}\alpha\,\alpha^3 e^{2ihv_1} \tag{35}$$

from Eq. (16), and with $R_p(\alpha) = -1$ for an ENZ medium. The traveling part comes from the integration range $0 \le \alpha < 1$. Here, we make the substitution $t = (1 - \alpha^2)^{1/2}$. This yields the representation

$$v_\perp(h)^{\mathrm{tr}} = -\int_0^1 \mathrm{d}t\,t(1 - t^2)\cos(\beta t). \tag{36}$$

Then, we expand $\cos(\beta t)$ in a series and integrate term by term. We then find the representation

$$v_\perp(h)^{\mathrm{tr}} = -\frac{1}{2}\sum_{n=0}^\infty \frac{1}{(2n)!(n+1)(n+2)}(-\beta^2)^n. \tag{37}$$

The first few terms are

$$v_\perp(h)^{\mathrm{tr}} = -\frac{1}{4} + \frac{1}{24}\beta^2 - \frac{1}{576}\beta^4 + \dots. \tag{38}$$

Along the same lines, we find

$$v_{\parallel}(h)^{\mathrm{tr}} = \frac{1}{8} + \frac{2}{15}\beta - \frac{3}{48}\beta^2 - \frac{4}{315}\beta^3 \ldots, \qquad (39)$$

and for the cross term, we obtain

$$v_{\times}(h)^{\mathrm{tr}} = \frac{2}{15}\beta - \frac{1}{105}\beta^3 + \ldots. \qquad (40)$$

For the cross term, the evanescent waves do not contribute, so the terms shown here are the dominant terms for $v_{\times}(h)$ at small distances. For $v_{\perp}(h)$ and $v_{\parallel}(h)$, the traveling contributions only produce slight wiggles in the curves for large distances.

8. EPSILON NEAR ZERO

The above results hold without approximation for the force on a dipole near an ENZ medium. For such a medium, $\varepsilon_r = 0$ (and $\mu_r = 1$). In practice, such a perfect ENZ material does not exist. The value of $\mathrm{Re}(\varepsilon_r)$ should be close to zero, and so should the value of $\mathrm{Im}(\varepsilon_r)$, in order to be considered ENZ material. We shall now consider the possible effects of small deviations from the perfect ENZ limit. We use the Fresnel coefficients from Eqs. (11) and (12), and the integrations in Eqs. (16)–(18) are performed numerically.

First, we consider the result for $v_{\perp}(h)$. Figure 6 shows $v_{\perp}(h)$ in the ENZ limit (solid line), which is the same curve as in Fig. 3. The dashed line is $v_{\perp}(h)$ for $\varepsilon_r = 0.5$. We see that the curve is somewhat shifted to the left, but the main features are the same. The corresponding force is still repulsive, but the magnitude of the force is slightly smaller for a given distance. When we set $\varepsilon_r = -0.5$, the curve shifts somewhat to the right, thereby increasing the force. When we set $\varepsilon_r = 0.5 * i$, representing damping in the material, there is hardly any change, as compared with the ENZ limit. The same conclusions hold for $v_{\parallel}(h)$.

For $v_{\times}(h)$, the force vanishes when the dipole gets close to the surface, as shown in Fig. 3. It also follows from Eq. (40) with $\beta \to 0$. Figure 7 shows the effect of a small positive value of ε_r. The lateral force no longer goes to zero for $h \to 0$, and the h dependence is significantly different than in the ENZ limit.

When we set $\varepsilon_r = -0.5$, the curve ends at a negative value for $h \to 0$.

More interesting is the effect of damping, as is illustrated in Fig. 8. Here, we took $\varepsilon_r = 0.01 * i$, and the change is dramatic. Even with this minuscule value of $\mathrm{Im}(\varepsilon_r)$, the value of $v_{\times}(h)$ diverges for $h \to 0$, just as it always does for $v_{\perp}(h)$ and $v_{\parallel}(h)$. The lateral force is $f_o v_{\times}(h)\mathrm{Im}[(\hat{\mathbf{u}}^* \cdot \mathbf{e}_z)\hat{\mathbf{u}}_{\parallel}]$, so, given $\hat{\mathbf{u}}$, its direction is determined by the sign of $v_{\times}(h)$. When we
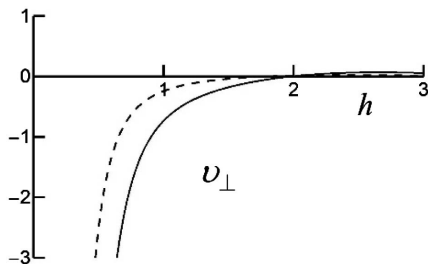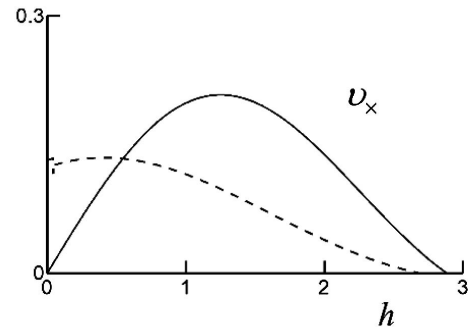
Fig. 7. Shown is $v_{\times}(h)$ in the ENZ limit (solid line) and for $\varepsilon_r = 0.5$ (dashed curve).
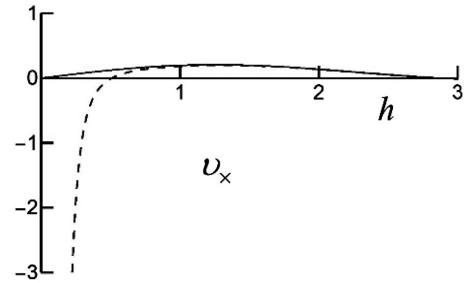
Fig. 8. Shown is $v_{\times}(h)$ in the ENZ limit (solid line) and for $\varepsilon_r = 0.01 * i$ (dashed curve).

take $\hat{\mathbf{u}}$ as in Eq. (19), we have $\mathrm{Im}[(\hat{\mathbf{u}}^* \cdot \mathbf{e}_z)\hat{\mathbf{u}}_{\parallel}] = -\mathbf{e}_y/2$, and because $v_{\times}(h)$ is negative, the force is in the positive y direction. Referring to the view in Fig. 1, the dipole moment rotates clockwise, and the lateral force is to the right.

It was shown above that $v_{\times}(h)$ has only a contribution from traveling waves in the ENZ limit. For $\mathrm{Im}(\varepsilon_r) > 0$, the evanescent waves kick in, such that the lateral force becomes large when the dipole is close to the interface. Practically, there will always be small damping in the material. Then, the lateral force becomes comparable with the perpendicular force, produced by the perpendicular and parallel parts of the dipole moment orientation vector $\hat{\mathbf{u}}$. In addition, there is lateral force by the laser beam, which illuminates the particle to induce the dipole moment. With $\hat{\mathbf{u}}$ from Eq. (19), this radiation must be circularly polarized and propagate along the x axis, as shown in Fig. 1. This radiation pressure force is in the propagation direction of the beam.

9. MIRROR

An ENZ material is as good as impenetrable for electromagnetic radiation. Only just below the surface, waves can travel along the surface as evanescent waves. No energy is transported into the material in the direction normal to the surface. It is tempting to speculate that this would lead to levitation [24]. The emitted radiation by the dipole in the downward direction has nowhere to go and produces a cushion for the particle. We shall now show that the mechanism for levitation is subtler.
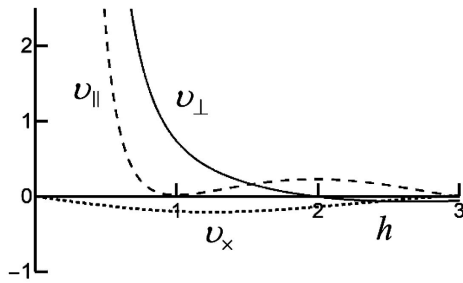
Fig. 6. Shown is $v_{\perp}(h)$ in the ENZ limit (solid line) and for $\varepsilon_r = 0.5$ (dashed curve).

Fig. 9. Figure shows the functions $v_\perp(h)$, $v_\parallel(h)$, and $v_\times(h)$ for a perfect conductor, as a function of h.

The ultimate impenetrable material is a perfect conductor (mirror). Not even evanescent waves can move below the surface through the material. In this mirror limit, the Fresnel coefficients are $R_s = -1$, $R_p = 1$. There is no dependence on the integration variable α, and the integrals in Eqs. (16)–(18) can be computed easily. We obtain

$$v_\perp(h) = -\frac{2}{\beta^2}\left[\left(1 - \frac{3}{\beta^2}\right)\cos\beta - \frac{3}{\beta}\sin\beta\right], \quad \textbf{(41)}$$

$$v_\parallel(h) = -\frac{\sin\beta}{\beta} + \frac{1}{\beta^2}\left[\left(\frac{3}{\beta^2} - 2\right)\cos\beta + \frac{3}{\beta}\sin\beta\right], \quad \textbf{(42)}$$

$$v_\times(h) = \frac{2}{\beta^2}\left[\frac{3}{\beta}\cos\beta + \left(1 - \frac{3}{\beta^2}\right)\sin\beta\right], \quad \textbf{(43)}$$

and Fig. 9 shows the corresponding curves. There is a striking resemblance between the curves in Fig. 9 for a mirror and the curves in Fig. 3 for an ENZ material. The graphs are almost identical but inverted with respect to the h axis. For $v_\perp(h)$ and $v_\times(h)$, this follows immediately from Eqs. (16) and (18). Only the Fresnel coefficient R_p appears in the expressions, and they are of opposite sign for a mirror and an ENZ material. For $v_\parallel(h)$, there is a slight difference between the ENZ result and the mirror result, although this can barely be seen in the figures. Clearly, when we have levitation for an ENZ medium, we must have attraction for a perfect conductor. The forces are as good as identical but of opposite signs. This shows that the difference between repulsion and attraction is determined by the phase shift upon reflection and not by expulsion of the radiation by the interface.

10. CONCLUSIONS

An electric dipole near an interface experiences a force by its own reflected radiation. We have derived a closed-form expression for this force for the case where the medium is an ENZ material. The result holds for any state of oscillation or rotation of the dipole moment. The force is (mainly) perpendicular to the surface, and it is shown that, for close (subwavelength) distances between the dipole and the interface, this force is repulsive. It is shown that the force is exerted on the dipole by the reflected evanescent waves of the angular spectrum of the radiation. The traveling waves only contribute minimally to some small wiggles for large distances. The force at close distances is proportional to h^{-4}, where h is the dimensionless distance

between the dipole and the surface (on such a scale, 2π corresponds to one optical wavelength). A cross term between the perpendicular and parallel components of the dipole moment appears in the expression for the force. For this term to contribute, the dipole moment needs to rotate (circle or ellipse) and have both a perpendicular and parallel component with respect to the surface. The resulting force is lateral (parallel to the surface), no matter the state or plane of rotation of the dipole moment. In the ENZ limit, this force only comes from the traveling waves in the angular spectrum and is, consequently, very small compared with the force perpendicular to the surface. However, when the slightest amount of damping in the material is present, this lateral force acquires a contribution from evanescent waves and becomes comparable with the normal force.

REFERENCES

1. Z. Xu and H. F. Arnoldus, "Reflection by and transmission through an ENZ interface," OSA Contin. **2**, 722–735 (2019).
2. M. G. Silveirinha and N. Engheta, "Tunneling of electromagnetic energy through subwavelength channels and bends using ε-near-zero materials," Phys. Rev. Lett. **97**, 157403 (2006).
3. M. G. Silveirinha and N. Engheta, "Theory of supercoupling, squeezing wave energy, and field confinement in narrow channels and tight bends using ε-near-zero metamaterials," Phys. Rev. B **76**, 245109 (2007).
4. A. Alù and N. Engheta, "Light squeezing through arbitrarily shaped plasmonic channels and sharp bends," Phys. Rev. B **78**, 035440 (2008).
5. D. A. Powell, A. Alù, B. Edwards, A. Vakil, Y. S. Kivshar, and N. Engheta, "Nonlinear control of tunneling through an epsilon-near-zero channel," Phys. Rev. B **79**, 245135 (2009).
6. B. Edwards, A. Alù, M. G. Silveirinha, and N. Engheta, "Reflectionless sharp bends and corners in waveguides using epsilon-near-zero effects," J. Appl. Phys. **105**, 044905 (2009).
7. A. Alù and N. Engheta, "Coaxial-to-waveguide matching with ε-near-zero ultranarrow channels and bends," IEEE Trans. Antennas Propag. **58**, 328–339 (2010).
8. S. Enoch, G. Tayeb, P. Sabouroux, N. Guérin, and P. Vincent, "A metamaterial for directive emission," Phys. Rev. Lett. **89**, 213902 (2002).
9. A. Alù, M. G. Silveirinha, A. Salandrino, and N. Engheta, "Epsilon-near-zero-metamaterials and electromagnetic sources: tailoring the radiation phase pattern," Phys. Rev. B **75**, 155410 (2007).
10. B. Wang and K.-M. Huang, "Shaping the radiation pattern with mu and epsilon-near-zero metamaterials," Prog. Electromagn. Res. **106**, 107–119 (2010).
11. L. V. Alekseyev, E. E. Narimanov, T. Tumkur, H. Li, Y. A. Barnakov, and M. A. Noginov, "Uniaxial epsilon-near-zero metamaterial for angular filtering and polarization control," Appl. Phys. Lett. **97**, 131107 (2010).
12. Z. Guo, F. Wu, C. Xue, H. Jiang, Y. Sun, Y. Li, and H. Chen, "Significant enhancement of magneto-optical effect in one-dimensional photonic crystals with a magnetized epsilon-near-zero defect," J. Appl. Phys. **124**, 103104 (2018).
13. B. Edwards, A. Alù, M. E. Young, M. G. Silveirinha, and N. Engheta, "Experimental verification of epsilon-near-zero metamaterial coupling and energy squeezing using a microwave waveguide," Phys. Rev. Lett. **100**, 033903 (2008).
14. H. Lobato-Morales, D. V. B. Murthy, A. Corona-Chávez, J. L. Olvera-Cervantes, and L. G. Guerrero-Ojeda, "Permittivity measurements at microwave frequencies using epsilon-near-zero (ENZ) tunnel structure," IEEE Trans. Microw. Theory Tech. **59**, 1863–1868 (2011).
15. V. Torres, B. Orazbayev, V. Pacheco-Peña, J. Teniente, M. Beruete, M. Navarro-Cía, M. S. Ayza, and N. Engheta, "Experimental demonstration of a millimeter-wave metallic ENZ lens based on the energy squeezing principle," IEEE Trans. Antennas Propag. **63**, 231–239 (2015).

16. M. Massaouti, A. A. Basharin, M. Kafesaki, M. F. Acosta, R. I. Merino, V. M. Orera, E. N. Economou, C. M. Soukoulis, and S. Tzortzakis, "Eutectic epsilon-near-zero metamaterial terahertz waveguides," Opt. Lett. **38**, 1140–1142 (2013).

17. V. Pacheco-Peña, N. Engheta, S. Kuznetsov, A. Gentselev, and M. Beruete, "Experimental realization of an epsilon-near-zero graded-index metalens at terahertz frequencies," Phys. Rev. Appl. **8**, 034036 (2017).

18. B. T. Schwartz and R. Piestun, "Total external reflection from metamaterials with ultralow refractive index," J. Opt. Soc. B **20**, 2448–2453 (2003).

19. R. Maas, J. Parsons, N. Engheta, and A. Polma, "Experimental realization of an epsilon-near-zero metamaterial at visible wavelengths," Nat. Photonics **7**, 907–912 (2013).

20. E. J. R. Vesseur, T. Coenen, H. Caglayan, N. Engheta, and A. Polman, "Experimental verification of $n = 0$ structures for visible light," Phys. Rev. Lett. **110**, 013902 (2013).

21. K. H. Drexhage, "Interaction of light with monomolecular dye layers," in *Progress in Optics XII*, E. Wolf, ed. (Elsevier, 1974), pp. 163–232.

22. J. A. Girón-Sedas, J. R. Mejía-Salazar, J. C. Granade, and O. N. Oliveira, Jr., "Repulsion of polarized particles near a magneto-optical metamaterial," Phys. Rev. B **94**, 245430 (2016).

23. F. J. Rodríguez-Fortuño, M. F. Picardi, and A. V. Zayats, "Repulsion of polarized particles from two-dimensional materials," Phys. Rev. B **97**, 205401 (2018).

24. F. J. Rodríguez-Fortuño, A. Vakil, and N. Engheta, "Electric levitation using ε-near-zero metamaterials," Phys. Rev. Lett. **112**, 033902 (2014).

25. L. Novotny and B. Hecht, *Principles of Nano-Optics* (Cambridge University Press, 2006), Chap. 13.

26. H. F. Arnoldus and M. J. Berg, "Energy transport in the near field of an electric dipole near a layer of material," J. Mod. Opt. **62**, 218–228 (2015).

27. F. J. Rodríguez-Fortuño, N. Engheta, A. Martínez, and A. V. Zayats, "Lateral forces on circularly polarizable particles near a surface," Nat. Commun. **6**, 8799 (2015).

28. M. Abramowitz and I. A. Stegun, *Handbook of Mathematical Functions* (Dover, 1972), Chap. 12.